Non-mean-field screening by multivalent counterions

M S Loth and B I Shklovskii

Department of Physics, University of Minnesota, Minneapolis, MN 55455, USA

E-mail: loth@physics.umn.edu

Abstract
Screening of a strongly charged macroion by its multivalent counterions cannot be described in
the framework of a mean-field Poisson–Boltzmann (PB) theory because multivalent counterions
form a strongly correlated liquid (SCL) on the surface of the macroion. It was predicted that a
distant counterion polarizes the SCL as if it were a metallic surface and creates an electrostatic
image. The attractive potential energy of the image is the reason why the charge density of
counterions decreases faster with distance from the charged surface than in PB theory. Using
the Monte Carlo method to find the equilibrium distribution of counterions around the
macroion, we confirm the existence of the image potential energy. It is also shown that, due to
the negative screening length of the SCL, -2ξ, the effective metallic surface is actually above
the SCL by $|\xi|$.

(Some figures in this article are in colour only in the electronic version)[1]

1. Introduction

In this paper we deal with a problem in which one large
and strongly charged ion, called a macroion, is screened by
much smaller but still multivalent counterions, each with a
large charge Ze (e is the proton charge); for brevity, we call
them Z ions. A variety of macroions are of importance in
chemistry and biology, including charged lipid membranes,
colloids, DNA and viruses. Multivalent metal ions such as
La^{3+}, dendrimers and short polyelectrolytes can play the role
of the screening Z ions.

To illustrate the fundamental aspects of screening we use
the simple geometry of a solid occupying the half-space $x \leqslant 0$,
whose surface at $x = 0$ has a large uniform surface charge
density $-\sigma$. The surface charge is screened by an aqueous
solution of positive, spherical Z ions with radius a, which
occupies the rest of space $x > 0$ (see figure 1). Both the
macroion and the aqueous solution have dielectric constant
$\epsilon \simeq 80$. If all of the Z ions were to condense on the macroion's
surface, their total charge per unit area would equal σ. In
such a neutral system, the concentration of Z ions $N(x) \to 0$
at $x \to \infty$. The main goal of this paper is to discuss the
behavior of $N(x)$. The solution of the Poisson–Boltzmann
(PB) equation for this problem has been known for nearly a

century [1, 2]. The Gouy–Chapman solution is

$$N(x) = \frac{1}{2\pi Z^2 l_B} \frac{1}{(\lambda + x - a)^2}, \qquad (1)$$

where $\lambda = e/2\pi\sigma l_B Z$ is the Gouy–Chapman length and
$l_B = e^2/(\epsilon k_B T) \simeq 0.71$ nm is the Bjerrum length. We have
modified the standard Gouy–Chapman formula, taking into
account the finite radius of the Z ions, which cannot approach
the surface closer than $x = a$.

It was shown [3–11] that the Gouy–Chapman solution fails
when both σ and Z are large enough. The reason it fails is that,
in addition to λ, there is a second length scale in the problem
due to the discreteness of charge. When the condensed Z
ions neutralize the charge of the plane, the two-dimensional
concentration of Z ions is $n = \sigma/Ze$, and the surface area
per ion, the Wigner–Seitz cell, can be approximated as a disc
of radius b such that $\pi b^2 = 1/n$. Thus, $b = (\pi n)^{-1/2} =
(Ze/\pi\sigma)^{1/2}$ and $2b$ is approximately the distance between Z
ions. We can construct the dimensionless ratio

$$\frac{b}{\lambda} = 2\Gamma, \qquad \Gamma = \frac{Z^2 e^2/\epsilon b}{k_B T}. \qquad (2)$$

Here Γ is the dimensionless Coulomb coupling constant or
the inverse dimensionless temperature measured in units of a
typical interaction energy between Z ions. For example, at
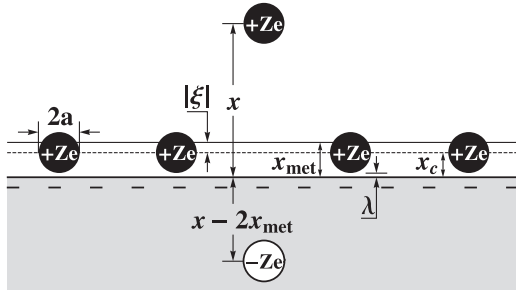
Figure 1. A stray positive Z ion (elevated black sphere) at a distance x from the surface (thick line) of a negatively charged planar macroion (shaded region). Other Z ions (black spheres), condensed at the surface, are on average a distance λ above the macroion's surface. The dashed line indicates the average distance, $x_c = a + \lambda$, from the macroion's surface to the adsorbed Z-ions' centers. The stray Z ion and its negative image charge (white sphere) are equidistant from the effective metallic surface, which is shown by the thin line at $x_{met} = x_c + |\xi|$.

$Z = 3$ and DNA like $\sigma = 0.95e$ nm^{-2} used in this paper, we get $\Gamma = 6.4$, $\lambda \simeq 0.79$ nm and $b \simeq 1.0$ nm. Thus, the Coulomb repulsion energy of the Z ions dominates the thermal energy. The result is a strongly correlated liquid, which has short-range order similar to a Wigner crystal [3–15] and is located, practically, at the very surface of the macroion. This paper deals only with the strong coupling case: $\Gamma \gg 1$. Another definition for a Coulomb coupling parameter, $\Xi = 2\Gamma^2$, was introduced in [9], and of course, in the limit $\Gamma \gg 1$, $\Xi \gg 1$ as well.

Mean-field treatments, along the lines of PB theory, fail at $\Gamma \gg 1$ since, when a Z ion strays away from the plane to distances $x - a \ll b$, the electric field of his neighbors has no significant $\hat{x}$ projection. In this range, the stray Z ion is only affected by the electric field of its Wigner–Seitz cell (a disc of radius b). Therefore, at $x - a \ll b$, the surface charge of the macroion is unscreened and the electric field is $2\pi\sigma/\epsilon$. Thus, for $0 < x - a \ll b$,

$$N(x) = \frac{\sigma}{Ze\lambda} \exp[-(x-a)/\lambda]. \tag{3}$$

(Here, following [5] we used an expression for $N(a)$ that ignores the atomic structure of water, while [3, 4] tried to take this structure into account.)

Remarkably, the same length λ characterizes both this exponential decay and the Gouy–Chapman solution, equation (1). It is clear that the dramatic difference between the exponential decay of equation (3) and the power law decay of equation (1) is due to the effects of correlations. Equation (3) was first obtained in [3, 4]. Then it was re-derived in [9, 10] and confirmed by Monte Carlo (MC) simulations in [11]. Below we again confirm equation (3) at $0 < x - a \ll b$ by MC simulations. However, the focus of this paper is on the non-PB behavior of $N(x)$ at larger distances $x - a > b$, which has been predicted in [3, 4] but to our knowledge has never been verified analytically or numerically.

To bring this prediction to mind, let us focus on a single, stray Z ion located above the macroion's surface at $x > a + b$

(figure 1). References [3, 4] argue that the negative charge of the correlation hole, $-Ze$, will spread to a disc of size $\sim x$ as neighboring Z ions move to occupy the Wigner–Seitz cell the stray Z ion left behind. This is similar to what happens in a metallic surface under the influence of an external charge. In fact, this metal-like polarization of the SCL on the surface of the macroion can actually be described by an image charge that appears in the body of the macroion. Because the centers of the Z ions which form the SCL are typically located at a distance $x_c = a + \lambda$ above the surface (see figure 1) it is natural to think that the effective metallic surface is at $x_{met} = x_c$ and therefore the image is located at $-x + 2x_{met}$. The attractive interaction energy between the stray Z ion and its image is then [16], for $x - x_{met} \gtrsim b$,

$$U_{im}(x) = -\frac{Z^2 e^2}{4\epsilon(x - x_{met})}. \tag{4}$$

This attractive image interaction, of course, is a correlation effect.

The goal of this paper is to verify, by a Monte Carlo (MC) simulation and an analytical calculation, that an SCL on the insulating surface of a macroion does behave as a metal, and a stray Z ion has potential energy $U_{im}(x)$. The plan of this paper is as follows. In section 2 we describe our MC procedure. In section 3, we present our MC results for the screening of a spherical macroion by Z ions. To a first approximation they confirm that a stray Z ion at $x > a + b$ has potential energy $U_{im}(x)$. This is the most important result of our paper.

At a more detailed level, we see in section 3 that to more accurately fit equation (4) to our MC data the effective metallic surface must be lifted slightly above x_c. We find that a shift of 0.21 nm provides the best fit. This shift is explained in section 4 where we analytically derive equation (4), showing that there is indeed an attractive interaction energy between the stray Z ion and its image. We further prove that the effective metallic surface should be lifted slightly by $-\xi = |\xi|$, where 2ξ is the linear screening length of the SCL. In other words, x_{met}, in equation (4), should be replaced by $x_{met} = x_c - \xi = x_c + |\xi|$. We show that, theoretically, $\xi = -0.20$ nm, in reasonable agreement with the MC simulation. The fact that a Wigner-crystal-like SCL has a negative screening radius was predicted theoretically [17] and confirmed experimentally for a low-density two-dimensional electron gas in silicon MOSFETs and GaAs heterojunctions [18, 19] (see also a recent paper [20]).

In section 5 we add a small concentration of monovalent salt (for example, NaCl) to our system. We show that the attractive image interaction persists in this system; however, the attraction is weaker due to screening.

2. Monte Carlo simulation

Our set-up is similar to the simulations found in [11, 21–25]. Our system is contained within a spherical cell with radius $r_{max} = 10.0$ nm. Centered within the cell is a spherical macroion with charge $Q_M = -300e$ and radius $R_M = 5.0$ nm ($-\sigma = -0.95e$ nm^{-2}). The system is populated by 100 Z ions of charge $3e$ and radius $a = 0.4$ nm. The mobile particles are

initialized to random non-overlapping coordinates. The wall of the spherical cell has a distance of closest approach of 0 so that a Z ion may be placed with its center at the wall. Therefore all Z ions are found at a radial distance r within the range $R_M + a < r \leqslant r_{max}$. After initializing the system, the total electrostatic energy of the system is calculated as

$$\mathcal{E} = \frac{e^2}{2\epsilon} \sum_{i,j;i \neq j}^{101} \frac{q_i q_j}{d_{ij}}, \qquad (5)$$

where particle i has charge q_i ($q_1 = Q_M$ and for $i > 1$, $q_i = Ze$) located at the center of a hard sphere with radius η_i ($\eta_1 = R_M$ and for $i > 1$, $\eta_i = a$). The distance between particles i and j is d_{ij}. The dielectric constant is set to $\epsilon = 80$ everywhere and there are no interactions with anything outside of the cell.

Selecting a particle at random, the MC program attempts to reposition it randomly within a cubic volume of $(3.2 \text{ nm})^3$ centered on the particle's current position. The total electrostatic energy of the system, $\mathcal{E}$, is calculated after each attempted move. Modeled as hard spheres, if any of the particles overlap after an attempted move, such that $d_{ij} < \eta_i + \eta_j$, the move is rejected. Additionally, any attempted move that places a particle outside of the cell, $r > r_{max}$, is also rejected. Otherwise, moves are accepted or rejected based on the traditional Metropolis algorithm. Simulations attempt 52 billion moves, of which ~4% are accepted, resulting in each particle being moved an average of 20 million times. This low acceptance rate is due to most of the Z ions being condensed on the macroion surface where their average separation is $b = 1.0$ nm; one can increase the rate to ~8% by shrinking the volume in which the Z ion is randomly repositioned to $(1.6 \text{ nm})^3$. To ensure thermalization, 5 million moves are attempted before beginning the analysis of $N(r)$, the Z ion's radial distribution.

Following thermalization, $N(r)$ is computed after every 20 000 attempted moves by dividing the simulation space around the central macroion into bins that are concentric spherical shells of thickness 0.1 nm, counting the ion population within each bin, and then calculating the average Z-ion density of each bin. We now introduce the empirical mean-field potential, $\phi(r)$, which corresponds to the MC $N(r)$ and is calculated from the radial distributions of the ions in the following way. First, the electric field is determined at the outer edge of each spherical shell by applying Gauss' Law to the integrated charge. Then, the potential $\phi(r)$ is calculated by discreetly integrating the electric field in the radial direction. The empirical mean-field potential, $\phi(r)$, has nothing to do with the PB potential obtained by a solution of the spherical PB equation because, due to correlation effects, the MC $N(r)$ differs from equation (1). In the present case, Z ions are strongly condensed at the surface of the macroion and therefore the potential $\phi(r)$ decays so fast with r that the interaction energy of a stray Z ion, $Ze\phi(r)$, becomes less than $k_B T$ already at $r > 5.65$ nm.

The main point of this paper is that the concentration of Z ions, $N(r)$, at a distance r from the center of the macroion, is only weakly influenced by the empirical mean-field potential
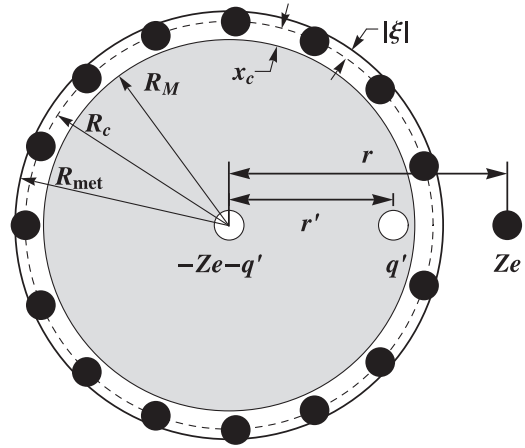
Figure 2. The generalization of figure 1 to a spherical geometry. A stray Z ion with charge Ze is shown in a cross-sectional view at a distance r from the center of a spherical macroion with charge Q_M, which is covered by condensed Z ions (black spheres). The condensed Z ions are located at an average distance of $R_c \equiv R_M + x_c = R_M + a + \lambda$ from the center of the macroion. The stray Z ion makes a correlation hole with charge $-Ze$, where the concentration of Z ions is depleted. The resulting correlation potential can be modeled as if the Z ion were near a metallic sphere with effective radius $R_{met} = R_c + |\xi|$. The image charges, $-Ze$ and $-q'$ located at the center and q' located at a distance r' away from the center, are shown by white spheres.

energy $Ze\phi(r)$ and is mostly determined by the attractive correlation energy $U_c(r)$. We extract $U_c(r) - U_c(r_{max})$ from the simulation data assuming that Z ions that stray from the macroion surface are Boltzmann distributed according to

$$N(r) = N(r_{max}) \exp \left(-\frac{Ze\phi(r)}{k_B T} - \frac{U_c(r) - U_c(r_{max})}{k_B T} \right), \qquad (6)$$

so that the change in the attractive correlation energy for a Z ion moved from r_{max} to r is

$$U_c(r) - U_c(r_{max}) = -k_B T \ln \left(\frac{N(r)}{N(r_{max})} \right) - Ze\phi(r), \quad (7)$$

where we took into account that $\phi(r_{max}) = 0$ because our system is neutral.

We need to recalculate the theoretical form of U_{im} for a spherical macroion geometry (see figure 2) to test that, for $r - R_{met} \gtrsim b$,

$$\Delta U(r) \equiv [U_c(r) - U_c(r_{max})] - [U_{im}(r) - U_{im}(r_{max})] = 0. \quad (8)$$

It is known [16] that a charge Ze at a distance $r > R_{met}$ from the center of a conducting sphere with radius R_{met} and a net charge of $-Ze$ induces two image charges within the sphere. The charge $q' = -ZeR_{met}/r$ is located at a distance $r' = R_{met}^2/r$ from the sphere's center and the compensating charge $-q'$ is located at the center of the sphere. The net charge of the macroion and the SCL, $-Ze$, accounts for the departure of the stray Z ion and is also fixed at the center of the sphere. In the presence of these three charges a stray Z ion, located at r, has potential energy given by

$$U_{im}(r) = -\frac{(Ze)^2}{r\epsilon} + \frac{Zeq'}{2(r - r')\epsilon} - \frac{Zeq'}{2r\epsilon}. \qquad (9)$$

The net charge $-Ze$ has fixed magnitude and position because, unlike charges q' and $-q'$, it is not created by the stray Z ion polarizing the SCL; therefore, the interaction term that involves the net charge does not include a factor of $1/2$. In the limit $x = r - R_M \ll R_M$, we recover the planar $U_{im}(x)$ of equation (4), because $U_{im}(r)$ is dominated by the influence of charge $q' \simeq -Ze$ located at $r' \simeq R_{met} - r$.

The first term within the parentheses of equation (9) is written for the case when all but one of the mobile charges (Z ions) are located, as in a metal, at the surface. This term then describes a stray Z-ion's attraction to the fraction of Q_M left uncompensated due to its departure. In other words, this term is used to exclude the stray Z-ion's self-interaction with its contribution to the mean-field potential[1].

To compare equation (9) to the simulation in the next section, we take $R_{met} = R_M + x_c \equiv R_c$, which aligns the metallic surface with the average position of the centers of the Z ions that comprise the SCL (see figure 2). Because our macroion is a sphere and not a plane, the magnitude of its electric field drops as $E \propto 1/r^2$ at $r > R_M$. Therefore, $E = 2\pi\sigma/\epsilon$, used to calculate λ, should be modified slightly since the Z-ion's centers are never closer than a to the macroion's surface. We introduce $\sigma_s = \sigma[R_M/(R_M + a)]^2$ to correct the electric field. This leads to $\sigma_s = 0.819e\,\text{nm}^{-2}$, $\lambda_s = 0.0913\,\text{nm}$, $\Gamma_s = 5.9$ and $R_{met} = 5.49\,\text{nm}$.
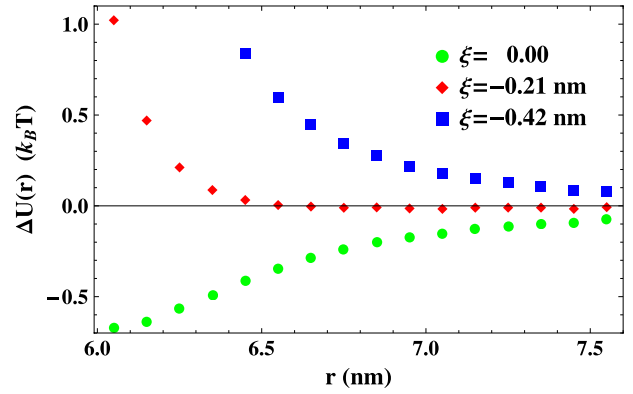
3. Results of MC simulation

$\Delta U(r)$ (equation (8)), the difference between the attractive correlation energy extracted from the MC simulation and the result of the image theory, is plotted in figure 3 for $R_{met} = 5.49\,\text{nm}$ (green circles). As expected, when $r - R_{met} \lesssim b$, i.e. at $r \lesssim 6.5\,\text{nm}$, the difference is significantly less than zero since in this range the SCL does not function well as a metal due to its discreteness and, therefore, the attractive correlation energy, $U_c(r)$, saturates. However, there is also weaker disagreement for $r \gtrsim 6.5\,\text{nm}$, which decreases with distance from the macroion. This suggests that we have improperly identified the radius of the effective metallic sphere used to calculate $U_{im}(r)$. To allow for the adjustment of R_{met}, we introduce the length $|\xi|$ so that

$$R_{met} = R_c + |\xi|. \tag{10}$$

By minimizing the root-mean-square of $\Delta U(r)$ with respect to $|\xi|$, on the interval $6.4\,\text{nm} \leqslant r \leqslant 7.4\,\text{nm}$, we determined that $|\xi| \simeq 0.21\,\text{nm}$ provides the best fit for $\Delta U(r) = 0$. The quality of this fit is illustrated in figure 3 (red diamonds). This small correction $|\xi|$ to R_c indicates that the foundation of equation (9), the attractive image interaction, is sound.

In section 4, we analytically calculate $U_{im}(x)$ in order to find the necessary adjustment in R_{met} by considering the response of a SCL, made up of adsorbed Z ions on a planar macroion, to the presence of a single stray Z ion above the

---

[1] Actually, $N(r)$ has a tail at $r > R_M + a$. As a result, when a stray Z ion is located at $r > R_M + a$, depletion of the mean distribution not only occurs at the surface of the macroion, but a small fraction, δ, of the total depletion also occurs at distances larger than r. For $r = 6.1\,\text{nm}$ this fraction is 0.02. As a result, the absolute value of this interaction energy is smaller than Z^2e^2/r by $\sim 2\%$. In equation (9) and below we neglect this small effect.

Figure 3. The difference, $\Delta U(r)$ (equation (8)), between the correlation attraction energy extracted from the MC simulation and the result of the image theory, as a function of a stray Z-ion's distance from the center of the macroion for three different values of the adsorbed Z-ion's screening length, 2ξ. The length, $|\xi|$, determines the increased radius, $R_{met} = R_M + a + \lambda + |\xi|$, of the effective metallic sphere used to calculate $U_{im}(r)$ (equation (9)). The green circles correspond to $\xi = 0$, assumed in the original theory of [3, 4]. The red diamonds correspond to the best fit to zero, $\xi = -0.21\,\text{nm}$. The blue squares correspond to $\xi = -0.42\,\text{nm}$ and are shown for comparison.

SCL. It is determined that the SCL screens the potential of the stray Z ion with a negative screening length, 2ξ, where $\xi = -0.20\,\text{nm}$. This moves the effective metallic surface further away from the macroion's surface by $|\xi| = 0.20\,\text{nm}$, in reasonable agreement with the MC data (see figures 1 and 2).

In figure 4, the concentration $N(r)$ obtained from the MC simulation is compared to

$$N(r) = N(r_{max}) \exp\left(-\frac{Ze\phi(r)}{k_B T} - \frac{U_{im}(r) - U_{im}(r_{max})}{k_B T}\right), \tag{11}$$

which uses $\xi = -0.21\,\text{nm}$ to calculate $U_{im}(r)$ (both $\phi(r)$ and $N(r_{max})$ are obtained from the MC simulation). The agreement between the MC data and equation (11) is obvious when $r \gtrsim 6.5\,\text{nm}$. In figure 4, we also compare equation (3), modified for a spherical geometry,

$$N(r) = \frac{\sigma_s}{Ze\lambda_s} \exp\left[-\frac{(r - R_M - a)}{\lambda_s}\right], \tag{12}$$

to the MC concentration data. At small distances, $r - R_M + a \lesssim b$, i.e. $r \lesssim 5.8\,\text{nm}$, we find good agreement with the exponential decay predicted in [3, 4] and confirmed in [9–11].

Let us now comment on what happens at larger distances from the macroion, which are not shown in figure 4 and cannot be studied well with the small size of the simulation cell used in this paper. According to [3, 4], at distances larger than

$$\Lambda = \left(\frac{e\lambda}{2\pi Z\sigma l_B}\right)^{1/2} \exp\left(\frac{|\mu|}{2k_B T}\right) \tag{13}$$

from the planar macroion the PB approximation takes over and

$$N(x) = \frac{1}{2\pi Z^2 l_B} \frac{1}{(\Lambda + x - a)^2}. \tag{14}$$
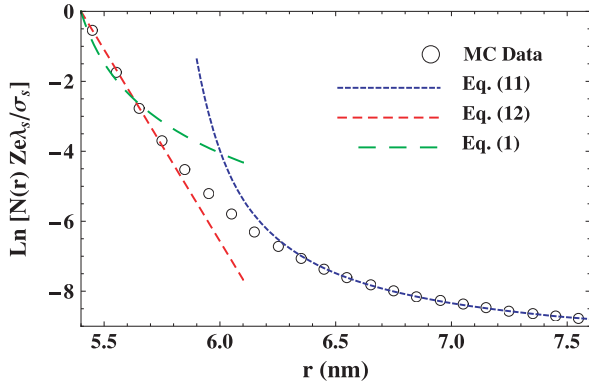
Figure 4. Concentration of Z ions, $N(r)$, as a function of distance from the center of the macroion, starting at $R_M + a = 5.4$ nm. The circles represent the data from the MC simulation. The result of the image theory, equation (11), is shown by short, blue dashes. The medium length, red dashes show equation (12). The long, green dashes show the Gouy–Chapman solution (equation (1)), with λ_s substituted for λ. The error bars for the MC data are smaller than the size of the symbols.

Here μ is the chemical potential of a Z ion in an SCL. It has been shown that for a SCL on a charged background (one-component plasma), at $1 < \Gamma < 15$, μ is approximated well by [4, 26]

$$\mu = -k_B T (1.65\Gamma - 2.61\Gamma^{1/4} + 0.26\ln\Gamma + 1.95), \quad (15)$$

where the first term of this expansion corresponds to the chemical potential of a Wigner crystal. For our parameters, $Z = 3$ and $\sigma = \sigma_s = 0.819e$ nm^{-2}, this leads to the length $\Lambda = 5.18$ nm. Then, the approximate extension of equation (14) to the spherical geometry using $x = r - R_M$ at $r = 7.55$ nm gives $\ln[N(r)Ze\lambda_s/\sigma_s] = -8.65$, very close to the MC result -8.77 (see figure 4). The idea behind the results of equations (13) and (14) is that the correlation physics at small distances $x - x_c \ll \Lambda$ produces a new boundary condition on the concentration of Z ions for the long distance solution of the PB equation [3, 4].

The authors of a recent paper [27] have already studied $N(r)$ at large distances by MC simulation in a much larger spherical cell and found that it is in agreement with the predictions of the PB approach based on the correlation driven boundary condition. They, however, did not identify the image domain of distances r which we concentrate upon here. Thus, all three asymptotic regimes, predicted in [3, 4], namely equation (3) at $x - a < b$, equation (4) at $b < x - a \ll \Lambda$ and equation (14) at $x - a > \Lambda$, are now confirmed by MC simulations.

We have shown above that the standard mean-field theory [1, 2] fails to describe screening by multivalent counterions. Let us now show that another mean-field approximation, which we call the empirical mean field, fails more dramatically. The empirical mean-field potential, $\phi(r)$, was introduced in section 2 and is obtained using the distribution of charge realized in our MC simulation. In figure 5, we compare the Z-ion concentration obtained from
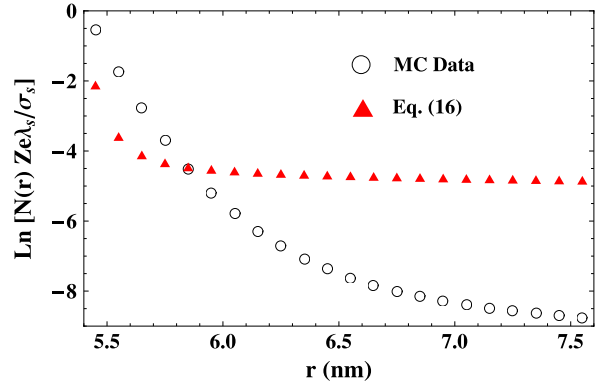
Figure 5. Concentration of Z ions, $N(r)$, as a function of distance from the center of the macroion. The MC concentration (circles; the same data as in figure 4) differs strongly from the concentration of Z ions (red triangles) obtained from equation (16) with the empirical mean-field potential $\phi(r)$.

the MC simulation to the Z-ion concentration predicted using the empirical mean-field potential:

$$N(r) = N_0 \exp\left(-\frac{Ze\phi(r)}{k_B T}\right). \quad (16)$$

Here, $N_0 = 2.18 \times 10^{-2}$ nm^{-3} is the concentration necessary to normalize the number of Z ions, in the range 5.4 nm $< r < 10.0$ nm, to 100. Clearly, the empirical mean-field potential is not self-consistent; equation (16) predicts that there are many more Z ions, at $r > 6.0$ nm, than are actually present in the distribution that produced $\phi(r)$. The distribution of the Z ions, for $r - R_{met} \gtrsim b$, is strongly influenced by the attractive correlation interaction and, therefore, cannot be predicted by the empirical mean-field interaction alone.

4. Theory of image potential and effective metallic surface

In this section we return to the plane geometry of figure 1 and analytically derive equation (4) for $U_{im}(x)$. In the process of this derivation, we find the theoretical location, x_{met}, of the effective metallic surface. The probe charge, a stray Z ion, is positioned far above the plane at $x' = x \gg b$ and $\varrho = 0$, where x' is the axis and ϱ is the radius of the cylindrical coordinate system (x', ϱ, θ). An SCL of Z ions is located in the (ϱ, θ) plane at $x' = x_c$, where the typical distance that separates adjacent Z ions is b.

The plan of this section consists of (1) determining the analytic solution for the total potential of the system, $\psi(\varrho, x')$, (2) presenting it as a sum of two potentials: one of the stray Z ion and the other of the induced charge density of the SCL, $\psi_{ind}(\varrho, x')$ (the potential of a point-like image) and (3) finding the position of the effective metallic plane, x_{met}, so that the attractive interaction energy $\frac{1}{2}Ze\psi_{ind}(0, x) = U_{im}(x)$. Below, we show that $x_{met} = x_c - \xi$, where 2ξ is the screening length of the SCL, which we also calculate.

To find the potential $\psi(\varrho, x')$ we solve Poisson's equation:

$$\nabla^2\psi(\varrho, x') = -\frac{4\pi}{\epsilon}\rho(\varrho, x'), \quad (17)$$

where $\rho(\varrho, x') = \rho_{ext}(\varrho, x') + \rho_{ind}(\varrho, x')$, with $\rho_{ext} = Ze\delta(\varrho)\delta(x' - x)/(\pi\varrho)$, and the charge density that is induced within the SCL is given by

$$
\begin{aligned}
\rho_{ind}(\varrho, x') &= Ze[n(\psi(\varrho, x_c)) - n(0)]\delta(x' - x_c) \\
&= Ze\psi(\varrho, x_c)\frac{dn}{d\psi}\delta(x' - x_c) \\
&= -(Ze)^2\psi(\varrho, x_c)\frac{dn}{d\mu}\delta(x' - x_c).
\end{aligned} \tag{18}
$$

Here, $n(\psi)$, is the number of Z ions per unit area as a function of the local total potential, $\psi(\varrho, x_c)$, and μ is the chemical potential of the SCL. We consider the case, $x - x_c \gg b$, when the stray Z ion produces a weak potential in the $x' = x_c$ plane ($Ze\psi(\varrho, x_c)/k_B T \ll 1$). This allows us to linearize ϱ_{ind} with respect to ψ, in equation (18). Rewriting equation (17) with the help of equation (18) results in

$$
\nabla^2\psi(\varrho, x') = -\frac{4\pi}{\epsilon}\rho_{ext}(\varrho, x') + \frac{1}{\xi}\psi(\varrho, x_c)\delta(x' - x_c), \tag{19}
$$

where

$$
\xi = \frac{\epsilon}{4\pi(Ze)^2}\frac{d\mu}{dn} = \frac{1}{2\kappa}, \tag{20}
$$

and κ is the inverse screening length of the SCL of adsorbed Z ions [20, 28].

In order to calculate ξ we use $\mu(n)$ as given by equation (15) and the definition of Γ from equation (2) and $b = (\pi n)^{-1/2}$. For $Z = 3$, $\sigma = \sigma_s = 0.819e$ nm^{-2} and $\epsilon = 80$, we find that $\xi = -0.20$ nm.

In order to solve equation (19) for $\psi(\varrho, x')$, we substitute

$$
\psi(\varrho, x') = \int_0^\infty k A_k(x') J_0(k\varrho)\,dk, \tag{21}
$$

into equation (19), where $A_k(x')$ are the coefficients of the expansion and $J_0(k\varrho)$ is the zeroth-order Bessel function. This yields [28]

$$
\begin{aligned}
\psi(\varrho, x') &= \frac{Ze}{\epsilon}\frac{1}{\sqrt{(x - x')^2 + \varrho^2}} \\
&\quad - \frac{Ze}{\epsilon}\int_0^\infty \frac{1}{2k\xi + 1}\exp[-k(x' + x - 2x_c)]J_0(k\varrho)\,dk.
\end{aligned} \tag{22}
$$

Because the screening length $\xi < 0$, the second term diverges. To obtain a solution despite this pole, following [20], we consider the contribution to $\psi(\varrho, x')$ from $k \ll 1/|\xi|$ only. Such an approach is valid if the stray Z ion, and the observation point x', are a large distance away from the SCL: $(x - x_c)$, $(x' - x_c) \gg |\xi|$. This allows us to expand $1/(2k\xi + 1)$ in equation (22) around $k = 0$, so that $1/(2k\xi + 1) \simeq 1 - 2k\xi$, and we arrive at

$$
\begin{aligned}
\psi(\varrho, x') &= \frac{Ze}{\epsilon\sqrt{\varrho^2 + (x - x')^2}} \\
&\quad - \frac{Ze}{\epsilon\sqrt{\varrho^2 + (x' + x - 2x_c)^2}} \\
&\quad + \frac{2(x' + x - 2x_c)Ze\xi}{\epsilon\left[\varrho^2 + (x' + x - 2x_c)^2\right]^{3/2}}.
\end{aligned} \tag{23}
$$

The first term of equation (23) is the potential created directly by the stray Z ion. The other two terms are the first two terms of the expansion of the induced potential, $\psi_{ind}(\varrho, x')$, with respect to ξ. We are now in a position to recast $\psi_{ind}(0, x)$ at $(x - x_c) \gg |\xi|$, as being created by an image charge a distance s below the stray Z ion:

$$
\begin{aligned}
\frac{1}{2}Ze\psi_{ind}(0, x) &= -\frac{(Ze)^2}{4(x - x_c)\epsilon} + \xi\frac{(Ze)^2}{4(x - x_c)^2\epsilon} \\
&\simeq \frac{(Ze)^2}{2s\epsilon} = U_{im}(x),
\end{aligned} \tag{24}
$$

where $s = 2(x - x_c + \xi)$. Specifying that the metallic plane must lie halfway between the real charge and the image charge sets its position at $x_{met} = x - s/2 = x_c - \xi$. Therefore the effective metallic plane is found a distance ξ above the plane of the adsorbed Z-ion's centers (figure 1). This agrees with the statement of [20] that the potential created by the stray Z ion is negative in the $x' = x_c$ plane. The theoretical value $\xi = -0.20$ nm is in reasonable agreement with our MC result, $\xi = -0.21$ nm (section 3). Moreover, we have demonstrated that the image attraction predicted in [3, 4] can be derived analytically in the limit $x \gg b$.

5. Screening the image by adding 1:1 salt

In this section we modify our system to include a small concentration of 1:1 salt molecules such as NaCl. By taking into account the effect of screening on the attractive interaction energy between a stray Z ion and its image, U_{im}, we obtain a new prediction for the concentration of Z ions, $N(r)$, which is in reasonable agreement with the new MC results. In calculating U_{im} we assume that the concentration c of 1:1 salt is so small that the total potential ψ at any point in the bulk solution ($r \gtrsim 6.0$ nm) obeys the linearized Poisson–Boltzmann equation:

$$
\nabla^2\psi = \kappa_b^2\psi, \tag{25}
$$

where $1/\kappa_b$ is the Debye–Hückel (DH) screening length:

$$
\frac{1}{\kappa_b} = \sqrt{\frac{\epsilon k_B T}{8\pi e^2 c}}. \tag{26}
$$

The exact solution of equation (25) for a point charge a distance $r - R_{met}$ away from the surface of a grounded metallic sphere in a weak electrolyte is known [29]; however, we will avoid the complexity of this solution and approximate the spherical macroion and its SCL as a grounded metallic plane. As seen in figure 6, where equation (4) is used to calculate $N(r)$ (short blue dashes) for $c = 0$, one obtains reasonable agreement with the MC $N(r)$ (circles) without using equation (9) as we did in section 3. This demonstrates that the influence of the total central charge, $-Ze - q'$, is very small. The reason for this is that, when a stray Z ion is close to the macroion surface, the total central charge is much smaller than the image charge q'. Additionally, the central charge is much further from the stray Z ion than the image charge q'. When the system includes 1:1 salt, the influence of the total central charge is further reduced due to screening.
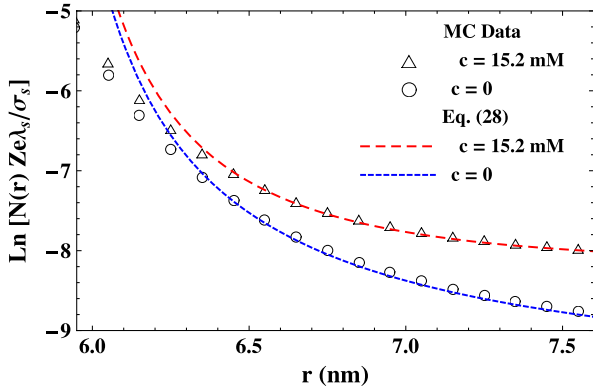
Figure 6. Concentration of Z ions, $N(r)$, in a weak electrolyte solution, as a function of distance from the center of the macroion. The shapes represent the data from the MC simulations for two different concentrations of 1:1 salt: 15.2 mM (triangles) and 0 (circles). The result of the screened image theory, equation (28) with $x = r - R_{met} + x_{met}$, is shown by medium length, red dashes for $c = 15.2$ mM and short blue dashes for $c = 0$. The error bars for the MC data are smaller than the size of the symbols.

Consider a Z ion which is submerged in a weak electrolyte solution with dielectric constant ϵ, and is a distance $x - x_{met}$ above a grounded metallic plane located at x_{met} (see figure 1). For this system, the solution to equation (25), subject to the boundary condition $\psi(x_{met}) = 0$, can be found using the method of images [29]. To satisfy the boundary condition, the image potential must exactly cancel the potential of our Z ion in the metallic plane. Such an image potential is provided by the DH screened potential of a charge $(-Ze)$ located at $x' = -x + 2x_{met}$.

The interaction energy of a stray Z ion with its screened image is now readily calculated and is given by

$$U_{im}(x) = -\frac{Z^2 e^2}{4\epsilon(x - x_{met})} \exp(-2\kappa_b[x - x_{met}]). \quad (27)$$

In the limit of infinite dilution $c \to 0$, or equivalently $\kappa_b \to 0$, equation (27) is equal to equation (4), as expected. Onsager and Samaras [30] obtained the same result, but with the opposite sign, for an ion's interaction with its image at an electrolyte–air interface resulting in a repulsive force. To compare equation (27) to the spherical geometry of our MC simulation, we take $x = r + x_{met} - R_{met}$ using $R_{met} = R_c + |\xi|$.

The MC simulation described in section 2 was modified to include M 1:1 salt molecules, resulting in M ions of charge e- and M ions of charge $-e$. All of the monovalent salt ions have their charge at the center of a hard sphere with radius $\eta = 0.2$ nm. We studied a 1:1 salt concentration of 15.2 mM corresponding to the addition of $M = 34$ salt molecules to the solution. The following changes were made to the MC simulation to properly incorporate the new ions. The sum used to calculate the total electrostatic energy of the system (equation (5)) was changed to include the monovalent ions, and the monovalent ions were also incorporated into the calculation of the empirical mean-field potential $\phi(r)$.

In figure 6, the concentration $N(r)$ obtained from the MC simulations is compared to

$$N(r) = N(r_0) \exp\left(-\frac{Ze[\phi(r) - \phi(r_0)]}{k_B T} - \frac{U_{im}(r) - U_{im}(r_0)}{k_B T}\right), \quad (28)$$

which uses $\xi = -0.21$ nm to calculate $U_{im}(x)$ (equation (27)) (both $\phi(r)$ and $N(r_0)$ are obtained from the MC simulations). Because there are no screening particles outside of the simulation cell, Z ions near the wall of the cell are repelled from this interface [31] even though there is no jump in the dielectric constant. To keep this effect separate from the image interaction of interest, we chose our reference point at $r_0 = 8.05$ nm instead of r_{max}. Because the stray Z-ion's attraction to the image is reduced by screening, we see that in figure 6 the concentration of Z ions is higher at distances $r > 60$ nm when 1:1 salt is present in the solution. Even with the addition of 1:1 salt to the solution the agreement between the MC data and equation (28) for $r \gtrsim 6.5$ nm is reasonable, demonstrating that the metallic behavior of the SCL on the macroion surface survives, and that the image attraction is still important in determining the Z ion's concentration.

6. Conclusion

To summarize, we have studied the role of correlations among adsorbed Z ions in attracting stray Z ions and influencing their distribution in the screening atmosphere. Adsorbed Z ions on the surface of the macroion form a strongly correlated liquid (SCL). The SCL acts as an effective metallic surface for Z ions that stray from the macroion surface to distances larger than the average distance between Z ions of the SCL. Using Monte Carlo (MC) simulations, we verified the theoretical prediction [3, 4] that a stray Z ion is attracted to its electrostatic image created behind the effective metallic surface. As a small correction to [3, 4], however, our MC simulation showed that the effective metallic surface is not aligned with the average position of the adsorbed Z-ion's centers, but is slightly above the adsorbed Z-ion's centers. This offset was calculated analytically to be $|\xi|$, where 2ξ is the screening length of the SCL. Our analytic theory is in reasonable agreement with the MC data. Extending the original image theory of [3, 4], we demonstrated that the attractive image interaction, while screened, persists in a weak monovalent electrolyte.

In [15] the attractive image interaction, which we have studied here, was used to interpret the origin of the negative chemical potential of the condensed Z ions (equation (15)). As a stray Z ion, attracted to its image, approaches the surface of the macroion it reaches a distance, $r \sim R_M + b$, where the SCL fails to act as a good metal and the correlation attraction $U_c(r)$ saturates at $\mu \sim -Z^2 e^2/4\epsilon b$; this saturation can be seen in figure 4 as the growth of $\Delta U(r)$ at $r < 6.5$ nm. It is this negative chemical potential, brought about by the attractive image interaction, at $r \gtrsim R_{met} + b$, which drives charge inversion (over-compensation of the macroion's bare charge with condensed Z ions), a phenomenon that has generated much interest [3–11]. Thus, we believe that this paper helps to clarify the origin of charge inversion.

Above, we have assumed for simplicity that the dielectric constant of the macroion and the surrounding water are the same, $\epsilon = \epsilon_w \simeq 80$. We now briefly consider a more realistic system where the macroion has a dielectric constant $\epsilon_m \ll \epsilon_w \simeq 80$, and we show that all of our results remain valid with very small corrections. For a single Z-ion a distance x above the planar interface of two dielectrics with $\epsilon_m \simeq 1$ for $x' < 0$ and $\epsilon_w \simeq 80$ for $x' > 0$, the Z-ion's interaction energy with its image, produced by the polarization of the dielectric, is given by

$$U_{d-im} \simeq \frac{Z^2 e^2}{4\epsilon_w x}. \tag{29}$$

Because of this repulsive image, the energy of a point like Z-ion is not a minimum at the surface of the macroion. Instead, it was shown in [15] that a point like Z-ion minimizes its energy a small distance away from the macroion. The finite radius of the Z-ions we have considered is larger than the optimum position calculated. Therefore, the position of a condensed Z-ion is not strongly affected by the smaller dielectric constant of the macroion.

For $r \gtrsim R_M + b$, we have demonstrated that the distribution of Z-ions in our system is determined mostly by their interaction with the effective metallic surface produced by the SCL. Upon introducing a macroion with $\epsilon_m \ll \epsilon_w$, the derivation presented in section 4, for the position of the effective metallic surface, must be modified to account for the new dielectric interface. The entire effect of the new dielectric interface can be accounted for by modifying the chemical potential (equation (15)), which determines the screening length of the SCL (equation (20)), and thus determines the position of the effective metallic surface (equation (24)). Corrections to the chemical potential (equation (15)) due to images formed by the macroion can be calculated as the interaction of the SCL with its image. In the Wigner crystal approximation this interaction was studied in [15, 32]. The interaction energy was shown to decrease exponentially with the distance between the SCL and its image. For a distance $\sim 2 \times 0.5$ nm $= 1$ nm, this interaction provides a small correction of less than 1% for the chemical potential (see equation (17) of [32] and equation (41) of [15]). This is why it is reasonable to extend the results of this paper to the case when $\epsilon_m \ll \epsilon_w$.

Acknowledgments

References

[1] Gouy M 1910 *J. Phys. Theor. Appl.* **9** 457
[2] Chapman D L 1913 *Phil. Mag.* **25** 475
[3] Perel V I and Shklovskii B I 1999 *Physica* A **274** 466
[4] Shklovskii B I 1999 *Phys. Rev.* E **60** 5802
[5] Grosberg A Yu, Nguyen T T and Shklovskii B I 2002 *Rev. Mod. Phys.* **74** 329
[6] Levin Y 2002 *Rep. Prog. Phys.* **65** 1577
[7] Boroudjerdi H, Kim Y W, Naji A, Netz R R, Schlagberger X and Serr A 2005 *Phys. Rep.* **416** 129
[8] Messina R 2009 *J. Phys.: Condens. Matter* **21** 113102
[9] Moreira A G and Netz R R 2000 *Europhys. Lett.* **52** 705
[10] Burak Y, Andelman D and Orland H 2004 *Phys. Rev.* E **70** 016102
[11] Moreira A G and Netz R R 2001 *Phys. Rev. Lett.* **87** 078301
[12] Rouzina I and Bloomfield V A 1996 *J. Phys. Chem.* **100** 9977
[13] Gronbech-Jensen N, Mashl R J, Bruinsma R F and Gelbart W M 1997 *Phys. Rev. Lett.* **78** 2477
[14] Shklovskii B I 1999 *Phys. Rev. Lett.* **82** 3268
[15] Nguyen T T, Grosberg A Yu and Shklovskii B I 2000 *J. Chem. Phys.* **113** 1110
[16] Landau L D, Lifshitz E M and Pitaevskii L P 1984 *Course of Theoretical Physics* (*Electrodynamics of Continuous Media*) 2nd edn, vol 8 (New York: Pergamon)
[17] Bello M S, Levin E I, Shklovskii B I and Efros A L 1981 *Sov. Phys.—JETP* **53** 822
[18] Kravchenko S V, Rinberg D A, Semenchinsky S G and Pudalov V 1990 *Phys. Rev.* B **42** 3741
[19] Eisenstein J P, Pfeifer L N and West K W 1992 *Phys. Rev. Lett.* **68** 674
[20] Efros A L 2008 *Phys. Rev.* B **78** 155130
[21] Lenz O and Holm C 2008 *Eur. Phys. J.* E **26** 191
[22] Diehl A and Levin Y 2006 *J. Chem. Phys.* **125** 054902
[23] Diehl A and Levin Y 2008 *J. Chem. Phys.* **129** 124506
[24] Quesada-Perez M, Martin-Molina A and Hidalgo-Alvarez R 2005 *Langmuir* **21** 9231
[25] Martin-Molina A, Maroto-Centeno J A, Hidalgo-Alvarez R and Quesada-Perez M 2008 *J. Chem. Phys.* **125** 124506
[26] Totsuji H 1978 *Phys. Rev.* A **17** 399
[27] dos Santos A P, Diehl A and Levin Y 2009 *J. Chem. Phys.* **130** 124110
[28] Ando T, Fowler A B and Stern F 1982 *Rev. Mod. Phys.* **54** 437
[29] Ohshima H 1994 *Adv. Colloid Interface Sci.* **53** 77
[30] Onsager L and Samaras N N T 1943 *J. Chem. Phys.* **2** 528
[31] Netz R R 1999 *Phys. Rev.* E **60** 3174
[32] Goldoni G and Peeters F M 1996 *Phys. Rev.* B **53** 4591